# *Ancient & Historic*
# METALS

## CONSERVATION AND SCIENTIFIC RESEARCH

*Proceedings of a Symposium*
*Organized by the J. Paul Getty Museum*
*and the Getty Conservation Institute*
*November 1991*

*Edited by*
DAVID A. SCOTT, JERRY PODANY, BRIAN B. CONSIDINE

THE GETTY CONSERVATION INSTITUTE

Symposium editors: David A. Scott, the Getty Conservation Institute; Jerry Podany and Brian B. Considine, the-J. Paul Getty Museum
Publications coordination: Irina Averkieff, Dinah Berland
Editing: Dinah Berland
Art director: Jacki Gallagher
Design: Hespenheide Design, Marilyn Babcock / Julian Hills Design
Cover design: Marilyn Babcock / Julian Hills Design
Production coordination: Anita Keys



Printed in Singapore

Library of Congress Cataloging-in-Publication Data
Ancient & historic metals : conservation and scientific research :
proceedings of a symposium organized by the J.-Paul Getty Museum and
the Getty Conservation Institute, November 1991 / David A. Scott,
Jerry Podany, Brian B. Considine, editors.
p. cm.
Includes bibliographical references.
ISBN 0-89236-231-6 (pbk.)
1. Art metal-work—Conservation and restoration—Congresses.
I. Scott, David A. II. Podany, Jerry. III. Considine, Brian B.
IV. J. Paul Getty Museum. V. Getty Conservation Institute.
VI. Title: Ancient and historic metals.
NK6404.5.A53 1995
730'.028—dc20 92-28095
CIP



*Cover photograph: Bronze sheathing tacks from the HMS Sirius. Courtesy of the Australian Bicentennial Authority. Photography: Pat Baker.*

**PICTURE CREDITS**

**Bassett and Chase** *Considerations in the Cleaning of Ancient Chinese Bronze Vessels.* Figures 1–4: Courtesy of the Honolulu Academy of the Arts, Honolulu. Photography: J. Bassett; Figure 5: Courtesy of the Arthur M. Sackler Gallery, Smithsonian Institution, Washington, D.C.; Figures 6–8: Courtesy of the Freer Gallery of Art, Smithsonian Institution, Washington, D.C.

**Bonadies** *Tomography of Ancient Bronzes.* Figure 1: Courtesy of Jason Franz; Figures 2–10: Collection of the Cincinnati Art Museum. Photography: Steve Beasley.

**Chapman** *Techniques of Mercury Gilding.* Figures 1–3: Courtesy of Maison Mahieu, Paris; Figures 4–5: © V&A Images/Victoria and Albert Museum, London. www.vam.ac.uk

**Chase** *Chinese Bronzes.* Figures 1–2: Courtesy of China Institute in America, Peter Lukic, after illustration in P. Knauth, *The Metalsmiths* (New York: Time Life Books, 1974, pp. 116-117); Figure 3: Courtesy of C. S. Smith. Photography: Betty Nielson, University of Chicago; Figures 4, 9–15, 17–21. Courtesy of the Freer Gallery of Art, Smithsonian Institution, Washington, D.C.; Figures 5–6: Data from Johnston-Feller 1991; Figure 7: Courtesy of Chen Yuyan, University of Science and Technology of China, from her work with Mike Notis, Lehigh University, Bethlehem, PA. Samples made for the Freer Gallery of Art by Rob Pond, Baltimore, MD; Figure 8: Study Collection, Freer Gallery of Art, SC-B-2. Photography: E. W. Fitzhugh; Figure 16: University of-Michigan Museum of Art, Ann Arbor. Estate of Oliver J. Todd, no. 1974/1.180.

**Grissom** *The Conservation of Outdoor Zinc Sculpture.* Figure 2: Courtesy of the Missouri HIstorical Society, St.-Louis; Figure 3: Courtesy, The Winterthur Library, Printed Book and Periodical Collection. Figure 7: Courtesy of John L. Brown Photo.

**Keene** *Real-time Survival Rates for Treatments of Archaeological Iron.* Figures 1–3: Courtesy Museum of London. Photography: the author.

**Lins and Power** *The Corrosion of Bronze Monuments in Polluted Urban Sites: A Report on the Stability of Copper Mineral Species at Different pH Levels.* Photography: A. Lins.

**Matero** *Conservation of Architectural Metalwork.* Figures 1, 2, 3, 10, 11: Courtesy of Ohio State University Archives.Figures 2, 10, 11: Photography A. Lins.

**MacLeod** *Conservation of Corroded Metals.* Figures 1–3: Courtesy of the Australian Bicentennial Authority. Photography: Pat Baker; Figure 4: Courtesy of the British Museum (Natural History), London.

**Marabelli** *The Monument of Marcus Aurelius.* Figure 1: Courtesy of Accardo, Amodio, et al. (1989); Figure 2: Courtesy of Accardo et al. (1985); Figures 5a–b and 6: Courtesy of Accardo et al. (1983). All photos courtesy of Ministero per i Beni e le Attività Culturali, Instituto Centrale per il Restauro, Roma.

**Ogden** *The Technology of Medieval Jewelry.* Figure 1: Courtesy of the York Museums Trust (Yorkshire Museum); Figure 2: Courtesy of the Trustees of the British Museum. Photography: N. Whitfield and K. East; Figure 6: Courtesy of W. Duckzo; Figures 8–13, 16, 17, 19, 20: Courtesy of the Trustees of the British Museum. Photography: the author; Figures 18, 22: Courtesy Fitzwilliam Museum. Photography: the author; Figure 23: Courtesy Cambridge Centre for Precious Metal Research archive.

**Oddy** *Gold Foil, Strip and Wire in the Iron Age of Southern Africa.* Figures 5, 18–21, 23–25: Courtesy of the Trustees of the British Museum; Figures 2, 6, 10, 11, 13, 14, 22, 26: Courtesy of Mapungubwe Museum, University of Pretoria; Figure 16: Courtesy of Queen Victoria Museum, Harare, Zimbabwe.

**Schrenk** *The Royal Art of Benin.* Figures 1, 2: Gift of Joseph H. Hirshhorn to the Smithsonian Institution in 1966. Photography: Jeffrey Ploskonka, National Museum of African Art; Figures 3, 4, 6, 8: Gift of Joseph H. Hirshhorn to the Smithsonian Institution in 1966. Photography: the author; Figure 5: Purchased with funds provided by the Smithsonian Institution Collections Acquisition Program in 1982. Photography: the author; Figure 7: Gift of Joseph H. Hirshhorn to the Smithsonian Institution in 1979. Photography: the author; Figure 9: Gift of Joseph H. Hirshhorn to the Smithsonian Institution in 1977. Photography: the author.

# The Monument of Marcus Aurelius: Research and Conservation

MAURIZIO MARABELLI

The equestrian monument of Marcus Aurelius, the most famous bronze monument of antiquity, is all that remains of the twenty-two *Equi Magni* that once adorned Late Imperial Rome. It was created according to the characteristic iconography of the so-called Type III style of the period following 161 C.E. and is thought to be connected with the celebration of a military victory of the emperor, perhaps in 173 C.E. (Fittschen 1989; Torelli 1989). The statue represents Marcus Aurelius with his right arm and hand in a relaxed pose, while his left hand is positioned as if holding the horse's reins, which are missing. The horse, of Nordic breed, is represented in the act of drawing up from a trot.

The gilt equestrian statue was probably erected in the area of the Fori and later moved to the Lateran Plaza, presumably in the eighth century following the political decline of the Imperial Fori. In the tenth century, according to the *Liber Pontificalis,* the *Caballus Constantini,* as the monument was then known, was visible in the Campus Lateranensis near the basilica of the same name and the patriarch's residence. This position corresponded to the new religious and political center of medieval Rome (De Lachenal 1989).

After the historical memory of Emperor Marcus Aurelius had been expunged, the monument first became a symbol of Constantine and papal authority. Then, in the twelfth century, according to the *Mirabilia Urbis Romae*, the statue was considered an effigy of a knight defending Rome against the barbarians. At the end of the twelfth century the statue probably underwent its first crude restoration. A further restoration certainly took place from 1466 to 1475 in at least two stages when the monument was placed on a new stone base, as shown in Filippino Lippi's fresco in the church of Santa Maria sopra Minerva (De Lachenal 1989). This restoration, carried out by the medalist Cristoforo Geremia da Mantova and the goldsmiths Corbolini and Guidocci, cost a total of 970 gold florins. About fifty years later, in January 1538, Paul III Farnese had the monument transferred to Capitoline Hill.

A new pedestal, commissioned from Michelangelo in 1539, was finally constructed in 1561 and is still visible today.

Two subsequent restorations took place, one in 1834–36 and another in 1912. The first was principally concerned with the static condition of the monument, while the second was an unscientific restoration of the surface with the addition of new dowels and the consolidation of preexistent patches and dowels (De Lachenal 1989).

In 1980 preliminary analyses of surface-corrosion products and an acoustic-emission and ultrasonics survey of the monument were carried out. The results of these tests revealed a defective structure and an extensive sulfur-dioxide attack on the surface (Marabelli 1979). In January 1981 the equestrian statue was moved to the Istituto Centrale per il Restauro (ICR) in San Michele, where it remained until the completion of the restoration in 1988. In December 1984 the results of the research were summarized in an exhibition and a catalogue (Aurelio 1984); other important results on casting and assembly techniques (Micheli 1989) and on gilding (Fiorentino 1989) were published subsequently.

The major investigations of the ICR laboratories preceding and accompanying the monument's most recent restoration included the following:

1. Static condition and structure of the monument
2. Nondestructive testing: fabrication and repair techniques
3. Analysis of the alloys
4. Thermal behavior of the monument
5. Climate and pollution: time of wetness and damage function
6. Patinas and types of corrosion
7. Process and condition of the gilding

## Static Condition and Structure

Evaluation of the static condition showed that the monument rests essentially on two of the horse's legs, the left-front and the right-back, while the left-back leg acts as a balance to the oscillations of the structure caused by wind, among other disturbances. The right-front leg is raised.

Structural examination of the monument and its tensile state was carried out or coordinated by the ICR Physics Laboratory, primarily using two different techniques: finite element mathematical (FEM) model and speckle interferometry. The purpose of these measurements was to assess the limits of stability of the bronze structure under the stress of its own weight.

Initially, the weights of the horse and horseman were calculated experimentally. The distribution of thickness was measured in each case, paying particular attention to the horse and what came to be considered its critical points (bearing legs and belly). Using a steel hook equipped with a strain-gauge element, the weight of the horseman was determined with reasonable accuracy to be 620 kg ± 6 kg (Accardo et al. 1984). The same technique was used to calculate the weight of the horse at approximately 1,300 kg.

Ultrasonics were used to determine the thicknesses of the metal. For example, the average thickness of the four legs was calculated as follows: left-front, 5.9 mm; right-front, 5.4 mm; left-back, 5.8 mm; and right-back, 5.8 mm. The average thickness of the belly measured 5.5 mm and 5.6 mm. Variations in thickness (standard deviations) were found to be fairly restricted (Table 1).

In order to develop a method for structural calculation of the finished elements, the form of the horse was reproduced on a computer by transferring the coordinates of the surface from photogrammetric images. The surface of the horse was subdivided into a grid structure corresponding to 365 shell elements, 406 nodes, and 36 high-stiffness beams. The schematic structure was then simulated for conditions of stress. The movements of the horse as a rigid body were calculated at considerable loads—in particular, under the weight of the horseman. The area that showed the most stress turned out to be the juncture of the left-front leg (Accardo, Amodio, et al. 1989). Figure 1 shows the movement of the mathematical model, magnified 109 times, as the horse moves forward and to the right under the weight of the horseman.

FEM model calculations were integrated with repeated linear measurements of displacement, using linear variable differential transformers (LVDT), of the raised front leg in all three directions. Calculations were also made with the application of

TABLE 1. *Statistical elaboration of the ultrasonic measurements of thickness (mm). (For symbols, see page 6.)*

| *Area* | *X* | *S* | *τ1* | *τ2* |
|---|---|---|---|---|
| Left-front leg | 5.9 | 1.3 | 0.3 | 1.8 |
| Right-front leg | 5.4 | 1.5 | 2.1 | 4.6 |
| Left-back leg | 5.8 | 1.0 | 0.7 | 5.7 |
| Right-back leg | 5.8 | 1.5 | 1.1 | 2.5 |
| Left side, repair | 5.2 | 1.2 | 1.0 | 1.9 |
| Left side, repair | 6.6 | 1.6 | −0.2 | −0.2 |
| Right side, repair | 5.1 | 1.2 | 0.8 | 2.6 |
| Right side, repair | 7.1 | 1.0 | 1.4 | −0.7 |
| Belly, left side, V1 | 5.4 | 1.1 | 1.5 | 9.3 |
| Belly, left side, V2 | 6.1 | 1.1 | −0.1 | 6.3 |
| Belly, left side, V3 | 6.6 | 1.5 | −2.4 | 2.5 |
| Belly, left side, V4 | 4.5 | 1.8 | 1.5 | −0.2 |
| Belly, left side, V5 | 4.9 | 1.2 | 1.1 | −0.1 |
| Belly, left side, Vt6, repair | 5.3 | 1.6 | 1.0 | −0.3 |
| Belly, right side, V7 | 6.1 | 1.4 | −0.05 | −0.6 |
| Belly, right side, V8 | 5.3 | 1.9 | −0.05 | −1.5 |
| Belly, right side, V9 | 5.3 | 2.0 | −0.1 | −1.5 |
| Belly, right side, V10 | 5.2 | 1.2 | 0.6 | 2.1 |
| Belly, right side, Vt11, repair | 6.7 | 2.2 | −0.1 | −0.1 |
| V1 + V2 + V3 + V4 + V5 = | 5.6 | 1.7 | 0.1 | −0.7 |
| V7 + V8 + V9 + V10 = | 5.5 | 1.7 | −0.2 | −0.8 |

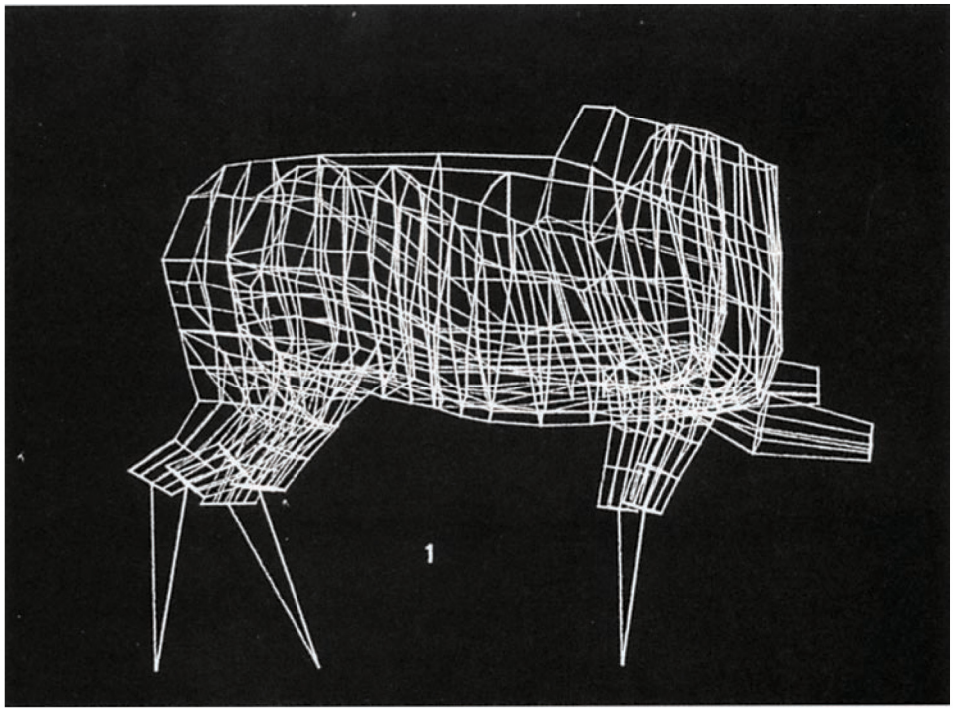


FIGURE 1. *Displacement of the horse under the weight of the horseman (×109).*

strain gauges (twenty-one groups of three elements), mostly attached to the inside of the left-front leg, and with the figure of the horseman placed on the horse in every experiment (Accardo, Bennici, et al. 1989). The greatest displacement of the left-front leg was concluded to be approximately 3 mm.

Among the possible hypotheses of attachment of the monument to its base, the one that corresponds to the minimum tension, according to the FEM model, presupposes a rigid fastening of the legs to the stone, with a forward displacement of the tip of the hoof of the left-front leg of 0.1% of the distance between this point and the corresponding back leg. This method of attachment would have been much easier to achieve than an internal framework of light, stiff metallic elements, which would have presented some difficulties in execution and maintenance (Accardo, Amodio, et al. 1989).

At the same time, the structural deformations of the horse were determined optically under a stress equal to approximately one-fourth the weight of the horseman. The structure was photographed with laser illumination (514.5 nm), first under the deformations caused by the added weight of the Marcus Aurelius, and later under normal conditions. This resulted in a kind of double exposure (Accardo et al. 1985). The photographic representation of a small area of the surface under laser illumination shows up on the film as an initial series of light and dark spots (speckles). A second series of spots corresponds to the first but is slightly displaced as a result of the deformations, producing a typical interference pattern (Young fringes).

The measurement of these displacements can be obtained by illuminating the photographic film with the same coherent light and measuring on a magnifying screen the period of the interference fringes that corresponds to the small selected area (in effect, measuring the distance between each successive fringe). From these data it is possible to determine the distance between two coupled speckles on the

FIGURE 2. *Speckle image of the neck and muzzle of the horse.*

film (d) and thereby the real displacement (L) of the structural deformation in the small area. Given the enlargement factor of the camera (M), d = ML.

Figure 2 shows the speckle image of the horse's neck and end muzzle, superimposed on the image of the surface illuminated with incoherent light; a series of segments corresponding to the displacements caused by elastic deformation of various microareas is visible. The length of the segments is proportional to the extent of the linear deformations (3 mm maximum) and their orientation to the direction of the displacements (Accardo et al. 1985).

One can deduce from these experiments that the structure of the monument, particularly that of the horse, undergoes a certain modest deformation in the elastic range when submitted to a force equal to the weight of the horseman. This is especially the case at the juncture of the left-front leg. Nevertheless the bearing legs easily withstand the weight of both statues, exhibiting a rather skillful casting under ultrasonics, showing uniform thickness reinforced with a tin-lead alloy filling.

The forces and subsequent deformations (elastic, for the most part) caused by weight, even when considered in the general context of other stresses to which the structure was submitted—such as thermal stress (discussed herein) primarily, and wind pressure (which can reach maximum values of about 57 kg/m$^2$) secondarily—never reach levels great enough to compromise the conservation of the monument.

Nevertheless, the numerous gaps, disjunctions, and irregularities of the structure, as well as the serious damage caused by relocations of the monument in past centuries, worried medieval conservators. These early restorers attempted, therefore, to displace some of the weight of the horseman onto two small stone columns that functioned in compression. The columns are visible in Pisanello's early fifteenth-century drawing of the left side of the monument (De Lachenal 1989). This drawing also shows a small column supporting the belly of the horse, perhaps intended to consolidate the structure at what was perceived to be the point of greatest stress.

## Nondestructive Testing

Nondestructive testing played a fundamental role in the preliminary phase of study. In addition, the data obtained were essential in determining the process by which the monument was fabricated.

The ICR Chemistry Laboratory examined the major sections of the two statues at more than 10,000 measurement points using ultrasonics. Researchers divided the surface into areas of smaller dimensions, subdivided each area into a grid of 2 cm squares, then transferred each value onto a flexible acetate sheet laid out along the curvatures of the surface.

Table 1 shows the thickness values of some areas with statistical values calculated, such as the standard deviation S, the curtosis $\tau 2$, and the skewness $\tau 1$, or asymmetry coefficient. The horse's four legs indicate remarkable homogeneity of casting, probably achieved by rotating the clay forms containing the molten wax. The overall average value of the thicknesses (x) of the entire bronze ranges from 5 mm to 6 mm, with minimums of 3 mm and maximums of 8 mm (Canella et al. 1985).

A radiographic survey (with 300 radiograms) by Micheli, together with endoscopic examination and direct observation, permitted the identification of the constituent sections. The statue of the horseman is made up of seventeen parts, separately cast and then joined together; the individual parts (head, arms, legs, and sections of drapery) were cast by the indirect, lost-wax method.

The horse is made up of fifteen sections (muzzle and neck, body in eight parts, legs, and tail), also cast separately by the same technique and then assembled (Micheli 1989). This was the most logical and simple process for casting bronzes of large dimensions, for which a single casting would have presented unmanageable difficulties. Not only the legs of the horse but also the other self-contained parts (the head, arms, and legs of the horseman) were obtained by pouring molten wax into a negative mold and distributing it by rotating the mold.

Radiograms have shown that the original sections underwent a slow process of cooling that, on one hand, prevented large cracks and cavities and, on the other hand, contributed to the separation of lead and slag into stratified bands in a frontal direction away from the solidification of the metal (Micheli 1989). The original solderings were made by pouring the molten metal directly and often discontinuously along the edges of the sections using, where possible, preexistent mechanical junctures.

The classification of the repairs to the monument proved rather complex. The first type of treatment, contemporaneous with the fabrication, was the filling in of missing parts, pores, and spongy areas in the cast with small (a few centimeters in diameter at most) rectangular dowels. Polygonal dowels of various sizes were also used in the same situations to repair either defects in casting or imperfections in the junctures between sections. A later type of repair, difficult to date, was used to fix extensive damage or large holes in the cast. In this method, cordlike strips of metal were used to join the cast with plates made to size, slightly smaller than the lacunae. The soldering was accomplished by pouring molten metal into the interior of the lost-wax casting. The molten-metal solder covered the edges of the juncture, forming

a cordlike strip that penetrated the interconnecting spaces between the cast walls and the repair plates laid against them. The same solder also penetrated the holes made in the original bronze and in the corresponding repairs to obtain a better mechanical adherence.

It is important to point out that the discontinuous Roman solderings and the later cordlike solderings do not correspond to continuous, structural welding, as in the hard-soldering process. Ultrasonic tests have verified without a doubt that there is no structural continuity between soldering strips and joints in the metal sections (Canella et al. 1985), as denoted by the low thickness values (Fig. 3); these are joints of a mechanical kind instead.

Other assembly and repair techniques from Roman times and later have also been identified. The classification of types of dowels, plates, plugs, and cordlike strips is especially difficult because of the reuse of older elements in later repairs and the superimposition of subsequent restorations.

Particularly useful in this investigation was an instrument for the measurement of conductivity expressed in International Annealed Copper Standard (IACS) percentages (Medori 1983). The conductivity of the metallic walls was measured to a depth of a few millimeters by means of a magnetic field. If the material under examination is copper, the measured value will correspond to the maximum range (100%); for copper, tin, and lead alloys, the value will decrease from 100%, diminishing in proportion to the increase in the noncopper components.

Using this technique, about 18,000 measurements were carried out, thus allowing the clarification of doubtful cases and the partial aggregation of results of the quantitative analyses of alloys, prior to statistical analysis (Fig. 4). By the end of the experimental survey, it was possible to conclude that the original sections and the Roman repairs revealed IACS% conductivity values generally equal to or below 13%,

FIGURE 3. *Thickness measurements of soldering with cordlike strips.*

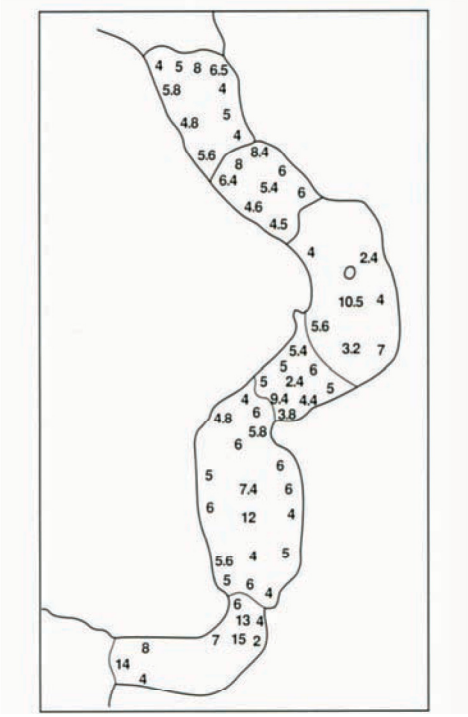

FIGURE 4. *IACS% conductivity measurements of original sections and repairs.*

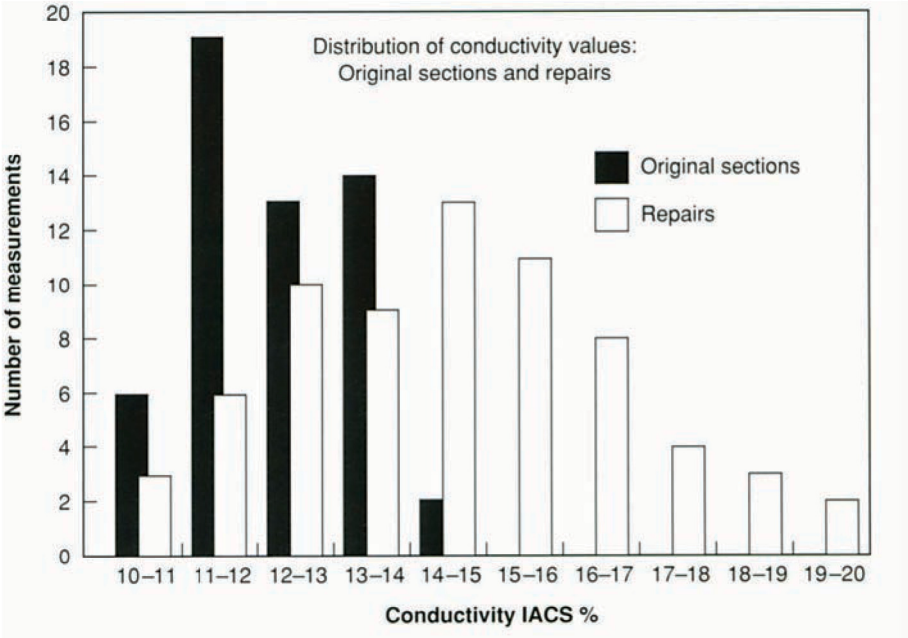

with some high points to about 15%, while the measurements of the later repair materials stayed mainly within a range of about 11–20%. The original sections of the horse and the horseman were chemically homogeneous, with rare exceptions.

## Analysis of the Alloys

Quantitative analysis of the alloys was based primarily on two methods:

1. Dispersive X-ray fluorescence analysis for the principal elements (Cu, Sn, Pb)
2. Plasma spectrography for secondary trace elements (Ag, Zn, Fe, Ni, Co, As, Sb, Bi, Si)

The first technique, used largely in archaeometry, does not require particular elucidation. However, in this specific case, an original method for the preparation of the sample was developed. It consisted of dissolving about 50 to 100 mg of alloy (25–50 ml final solution), depositing 200 microliters onto a paper filter (ϕ 14 mm), and analyzing the spectrum of X-ray fluorescence obtained by the irradiation of the filter with a target of barium acetate excited by a primary X-ray source, Bα Kα = 32 KeV (Ferretti et al. 1989).

In plasma-emission spectrometry, the sample is introduced in aerosol form, into a flow of ionized argon at a range of 10,000–12,000 °C. Given the high temperature and the subsequent high level of excitation, sensitivities on the order of parts per billion or milligrams per liter are reached.

About one hundred specimens were studied in all. On initial examination the matrix of percentage values was difficult to interpret. Therefore, the values were reexamined and sequenced in light of two criteria: (1) the sources and analytical data available in the literature, and (2) the statistical elaboration of the data.

A very important passage on the description of bronze alloys used by the Romans, albeit somewhat ambiguous in part, is found in the *Natural History* of Pliny the Elder, book XXXIV, chapter 20 (1961:95–98). Pliny lists five types of bronze alloys: (1) *campana,* an alloy used for vases and utensils; (2) an alloy similar to the previous one, used for the same purposes; (3) an alloy for statues and bronze plaques; (4) *tenerrima,* an alloy for casting statues in molds; and (5) *ollaria,* an alloy for making vases.

Table 2 lists the components of these alloys according to Pliny's categories without interpretation. In the last few years, three interpretations have been given to the term *plumbum argentarium* cited by Pliny. According to Caley (1970), it is a 50/50 lead-tin alloy (Table 3). However, this interpretation seems unfounded, as Pliny refers to an alloy used for counterfeits, which "some call *argentarium*" (1961:95–98).

A second interpretation (Picon et al. 1967) identifies *plumbum argentarium* with tin (Table 4). This identification appears to be well founded because of the noticeable absence of tin in all of the alloys cited by Pliny, and because this interpretation may allow the different compositions to be typed and differentiated, as Picon et al. show rather clearly in two other publications (1966, 1969).

TABLE 2. *Alloys described by Pliny (1961).*

| *Alloy* | *aes* | **a.c.* | ***p.a.* | ****p.n.* | *plumbum* |
|---|---|---|---|---|---|
| 1. *Campana,* bronze alloy for vases and utensils | 90.9 | | 9.1 | | |
| 2. Alloy similar to the previous one | 92.6 | | | | 7.4 |
| 3. Alloy for statues and bronze plaques | 68.6 | 22.8 | 8.6 | | |
| 4. *Tenerrima,* alloy for casting statues in molds | 87.0 | | 4.3 | 8.7 | |
| 5. *Ollaria,* alloy for vases | 96.2–97.1 | | 2.9–3.8 | | |

*a.c. = *aes collectaneum*

**p.a. = *plumbum argentarium*

***p.n. = *plumbum nigrum*

TABLE 3. *Pliny's alloys according to Caley (1970).*

| *Alloy* | *Copper* | *Tin* | *Lead* |
|---|---|---|---|
| 1 | 90.9 | 4.5 | 4.5 |
| 2 | 92.6 | 7.4 | |
| 3 | 86.8 | 6.6 | 6.6 |
| | 81.2–81.3 | 8.7–9.7 | 9.1–10.0 |
| 4 | 81.4 | 6.8 | 11.8 |
| | 72.7 | 7.8 | 19.5 |
| 5 | 96.2–97.1 | 1.4–1.9 | 1.4–1.9 |

TABLE 4. *Pliny's alloys according to Picon et al. (1967).*

| *Alloy* | *Copper* | *Tin* | *Lead* |
|---|---|---|---|
| 1 | 90.9 | 9.1 | |
| 2 | 92.6 | 7.4 | |
| 3 | 87.0–89.0 | 11.0–13.0 | |
| 4 | 86.9 | 4.4 | 8.7 |
| 5 | 96.2–97.1 | 2.9–3.8 | |

The third hypothesis by the *Projektgruppe Plinius* (Plinius der Ältere 1984) identifies *plumbum argentarium* with lead (Table 5). This interpretation encounters two difficulties: First, tin does not appear as an alloy component, which would require an alloy containing tin to be identified with the term *aes* in every case. Second, in the formula for statuary bronzes (alloy no. 4) lead would have to be added and named twice—as *plumbum nigrum* and as *plumbum argentarium,* respectively—without substantial difference and therefore without apparent reason.

Nevertheless this very formula of no. 4 (13% Pb) should be very close to the lead-bronze formula commonly used by the Romans for sculptural works, according to a technical tradition that dates back to the fourth century B.C.E. It is probable that the use of lead bronze was slow to be accepted because the characteristics caused by

TABLE 5. *Pliny's alloys according to the* Projektgruppe Plinius *(Plinius der Ältere 1985).*

| *Alloy* | *Copper-bronze* | *Lead* |
|---|---|---|
| 1 | 90.9 | 9.1 |
| 2 | 92.6 | 7.4 |
| 3 | 68.6 + 22.8 | 8.6 |
| 4 | 87.0 | 13.0 |
| 5 | 96.2–97.1 | 2.9–3.8 |

the addition of lead to bronze alloys were not well known. In fact, large quantities of this metal led to the phenomenon of liquation and to the development of discolored patinas.

It is also likely that from the fourth century B.C.E. on, a technical tradition developed for the use of lead in controlled quantities in statuary, taking advantage of the metal already available on the market as a by-product of silver-working. This would explain an interesting observation concerning the statistical interpretation of the data. The results of the quantitative analysis were interpreted for various groups in order to obtain the average value, the standard deviation, the coefficients of correlation between the various elements, and the levels of statistical significance. Statistical elaboration of the data was carried out on characteristic groups of values corresponding to the types of alloys already identified by means of the preceding chemical analyses and nondestructive tests.

The logical process of the research may be summarized as follows: nondestructive testing plus visual examinations, initial identification of the alloys, sampling and chemical analysis, testing with measurements of conductivity IACS%, classification of analytical data in groups, and statistical analysis of the groups.

Several interesting conclusions can be drawn from the final results of statistical analysis, only partially shown in Table 6. First, the original sections show a negative correlation between copper and lead (−0.79), while there is no correlation between tin and either copper or lead. The standard deviation relative to the percentage concentrations of lead is relatively low. From this, one could deduce that the ancient founder was concerned about keeping the lead within a "safe" percentage by applying a formula of reference of the type:

$$100 - \text{lead} = \textit{aes} + \textit{aes collectaneum} \text{ (scrap copper and bronze)} + \text{tin}$$

The tin does not correlate with copper and lead, probably because the percentage of tin in the *aes collectaneum* varied each time without a systematic point of reference.

Second, the addition of lead confers some specific characteristics on the alloy: the fusion point of the alloy diminishes and the cast becomes more fluid, while the surface of the bronze becomes more workable and polishable with scrapers, files, and pointed tools (although the workability by hammering declines).

Third, the absence of correlations between the other alloy elements shows that the various original sections, cast separately, were made with metal from different stocks, probably also using *aes collectaneum*.

TABLE 6. *Statistical analysis of the original (Roman) alloys of the* Marcus Aurelius.

| | *Average %* | | | *Standard deviation %* | | | *Minimum–Maximum %* | | |
|---|---|---|---|---|---|---|---|---|---|
| *Alloy* | *Cu* | *Sn* | *Pb* | *Cu* | *Sn* | *Pb* | *Cu* | *Sn* | *Pb* |
| Roman sections | 80.7 | 6.8 | 12.0 | 2.57 | 1.44 | 2.32 | 75.9<br>85.6 | 3.9<br>10.5 | 8.4<br>16.4 |
| Roman soldering | 74.0 | 6.6 | 19.4 | 1.75 | 2.16 | 1.74 | 71.6<br>77.0 | 3.8<br>10.2 | 16.9<br>23.1 |

Table 6 shows the statistical values for twenty-eight original Roman alloy specimens and for ten specimens of Roman soldering. For soldering, no correlation was found between copper, tin, and lead, suggesting a rather approximate mixture of principal components, the only restriction being that the cumulative percentage of tin plus lead must not drop below a certain level. In this case, the lead not only lowers the melting point and viscosity of the alloy but also acts as a true deoxidant for the soldering, forming with the tin dioxide ($SnO_2$) a compound ($Pb_2SnO_4$) that melts at 1060 °C (Steinberg 1973; Lechtman and Steinberg 1970).

The elaboration of the data for the repaired sections was still in progress in early 1992, with some difficulties of interpretation because of the great variety of alloys used for restoration (in collaboration with E. D'Arcangelo).

## Thermal Behavior of the Monument

One particularly interesting area of study has been that of the environmental causes of deterioration. The exchange of thermal energy between the environment and the monument has been thoroughly investigated, revealing that the mechanical stresses suffered by the bronze in its position on Capitoline Hill have also been dependent on the daily cycles of expansion and contraction of the metal structure. A description of the thermal behavior of the material is useful for a better understanding of an important series of problems that are not only mechanical but also involve the electrochemical and chemical corrosion of the surface.

The Piazza del Campidoglio is located about twenty meters above traffic level and is enclosed on three sides by the Palazzi Capitolini. The monument of Marcus Aurelius is placed in the center and oriented toward the northwest by 60°; that is, toward the wide ramp designed by Michelangelo. The particular placement of the monument and the geometry of the plaza allow direct sunlight to strike the metallic surface unevenly, warming different sections of the bronze at different hours of the day. In order to analyze the thermal exchange between the monument, its stone base, and the surrounding air, continuous readings of the surface temperature in ten areas were taken during the summer, along with thermovision images of the monument. At the same time, a series of acoustic-emission measurements were taken to register incidents of deformation in the horse over a 24-hour period (Accardo et al. 1983).

This last technique, in particular, operates on the principle that structural deformations and the formation or increase of cracks release microquantities of elastic

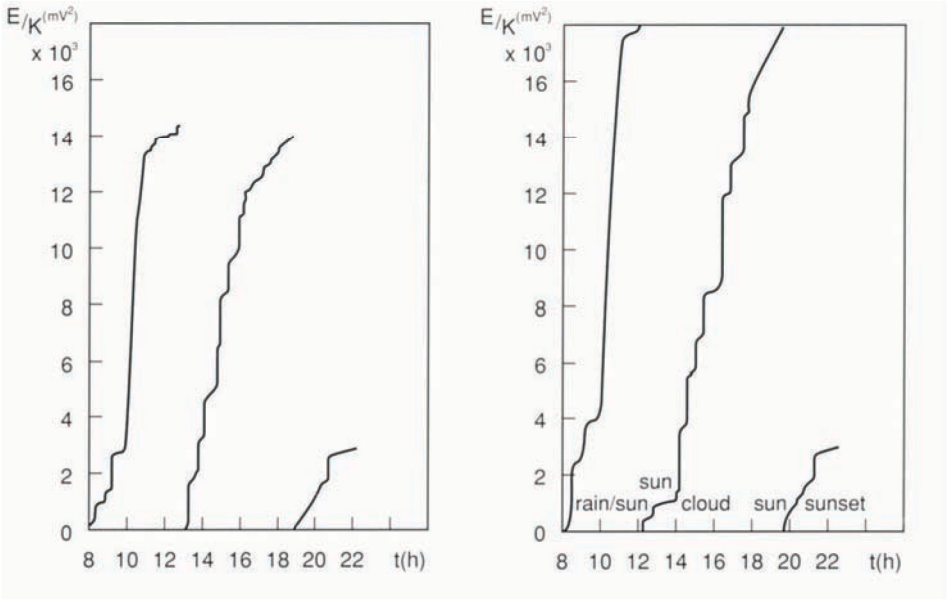


FIGURE 5a, b. *Registration of acoustic emission on (a) a clear day; and (b) a cloudy day.*

energy, causing propagation of mechanical pressure waves at a frequency greater than 10 MHz, which are picked up by a piezoelectric transducer and stored and analyzed by a sequential electronic apparatus.

Using these techniques, several important findings have emerged. First, the horse's left-front leg showed particular stress from direct solar radiation after ten o'clock in the morning. Of the two registrations in Figures 5a and 5b, the first shows the course of energy emitted on a clear day, while the second represents the phenomenon on a cloudy day with rain. It is evident that more energy is released under conditions of maximum irradiation as well as during rapid variations of surface temperature.

Second, because of its greater thermal inertia, the stone base maintains a surface temperature higher than that of the bronze alloy and keeps the lower part of the horse warmer during the night, while the hindquarters cool down through radiant emission toward the sky (Fig. 6).

In general the bronze surface responds quickly, because of its scant thermal inertia, to the temperature variations of the surrounding air. Exceptions may include the legs, which are filled with a lead-tin alloy (*metallone*) and the belly of the horse, because of its thermal exchange with the stone base. The thermovision images of the legs are certainly influenced by the greater thermal capacity of the volumes filled with lead-tin alloy, which show up as lighter (i.e., hotter), while the dark areas correspond to "empty" spaces (Accardo et al. 1983).

From the structural point of view, one may conclude that the low level of energy released by the structure corresponds to incidents of temporary (elastic) deformation, particularly involving that section of the left-front leg of the horse already subject to the mechanical stresses of the monument's weight.

Finally, in regard to the electrochemical aspects, climate certainly has a decisive influence on the kinetics of the bronze's corrosion. Given the rapid adjustment of the metal surface to the temperature of the surrounding air, the events of precipitation and capillary condensation are the primary elements that accelerate electrochemical corrosion.

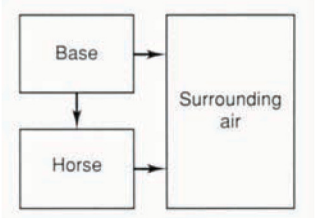


FIGURE 6. *Nocturnal heat exchange between the air, the monument, and the base.*

In recent years damage functions have been developed to calculate the electrochemical corrosion of a metal object over the course of a year, taking into account the amount of time the surface remains wet and the integrated fluxes of deposition of the more destructive airborne pollutants. For the Roman climate, the time of wetness (*tw*) of a metallic surface exposed outdoors is given as:

$$tw = tw1 + tw2$$

where *tw*1 equals the time of wetness of the surface caused by rainfall and *tw*2 equals the time of capillary condensation (Marabelli et al. 1988). Capillary condensation is linked to the shape and diameter of capillary pores in the patina and starts at a relative-humidity value well below 100% (corresponding to traditional surface condensation).

In order to measure the threshold value of relative humidity corresponding to the beginning of capillary condensation, the ICR Chemistry Laboratory developed a prototype consisting of an automated apparatus programmed by computer and capable of measuring surface conductivity and volume conductivity of patinas, which is variable in terms of relative humidity (Marabelli et al. 1988). This instrument comprises a measurement cell of conductivity, which clings to the metal surface and within which a particular hygrometric progression is produced in a predetermined way.

In the case of the Marcus Aurelius, by increasing the relative humidity (RH), it was possible to document, after some 160 experiments, that the surface conductivity increases rapidly above approximately 80% RH (Marabelli et al. 1988). Figure 7 shows a typical experimental curve corresponding to the surface electrical conductivity function, *f*(RH). The resulting theoretical function is:

$$y = 0.8 \cdot \exp\left(-\left[80-x\right] / 3\right)$$

where *y* equals the conductivity in microsiemens and *x* equals RH.

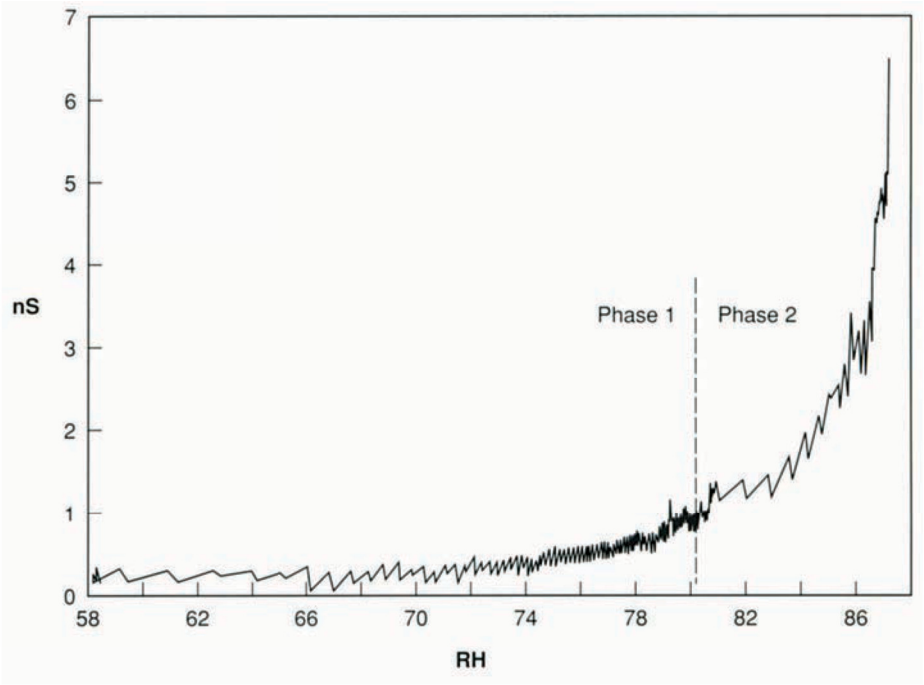


FIGURE 7. *Surface conductivity dependent on relative humidity.*

Knowing the daily distribution frequency of relative humidity over the course of a year, it was possible to determine that *tw*2 equals approximately 22.8 days, while *tw*1 can be roughly deduced from the monthly averages of pluviometric data for the historical center of Rome over a 10-year period. The total *tw* equals approximately 0.22 per year. This finding was used to calculate the corrosion velocity of the monument exposed outdoors by using a damage function developed by Benarie and Lipfert and slightly modified for this specific case (Marabelli 1992). The velocity of electrochemical corrosion, *Vc,* expressed in g/m$^2$ per year, equals:

$$Vc = tw \cdot 0.38 \cdot a\ (f\mathrm{SO}_2 + 1.1 \cdot f\mathrm{Cl}^-)$$

where tw equals the total annual time of wetness; *a* equals the dilution factor of the pollutants, taking into account the elevated position of the plaza; and $f\mathrm{SO}_2$ and $f\mathrm{Cl}^-$ equal the integrated fluxes of deposition expressed in mg/m$^2$ per day.

As a result, it was possible to determine the velocity value of the electrochemical corrosion of the alloy at roughly 0.2 microns per year (Marabelli 1992). It would seem possible to extrapolate from these data encouraging indications for the conservation of the Marcus Aurelius outdoors. However, it must be remembered that the chemicophysical corrosion of the patina, caused by airborne acidic pollutants as well as rainfall, still causes a constant erosion of the surface with loss of gilding.

To better understand the conditions of the formation and transformation of corrosion products in relation to the climate and other environmental parameters in the broad sense, a series of samples of the patina differentiated by color, consistency, and orientation to sunlight and rainfall was taken and examined using X-ray diffraction.

## Patinas and Types of Corrosion

The surface of the Marcus Aurelius reveals extensive sulfation, with the formation not only of brochantite but also antlerite and chalcanthite, a soluble copper sulfate. Since brochantite is stable between 3.5 and 6.5 pH, and antlerite is stable between 2.8 and 3.5 pH, the presence of the chalcanthite indicates that the pH level on the surface of the monument must have fallen below 2.8, probably as a result of microcondensation (Graedel 1987).

The partial dissolution of the patina evidently makes the already precarious mechanical adhesion of the gold even more unstable, to the point that even the application of a fixative may cause damage to the gilding. Furthermore, the gilding always appears so fragmentary and riddled with holes that water easily infiltrates the underlying patina (Fig. 8). The areas protected from the driving rain and from water runoff appear darker due to the accumulation of carbon substances and other components of the atmospheric particulate (gypsum, feldspars).

Conversely, the horizontal surfaces facing upward and those corresponding to the geodetic lines of rainwater appear lighter because of the absence of carbon particles. The alternation of darker (cathodic) stripes and lighter (anodic) stripes on the flanks of the horse form a typical zebra pattern (Fig. 9). Spots and whitish stains along with gray patinas covering the gold are rich in anglesite, present along with

brochantite in almost all the samples. A few areas of the monument bear traces of a brownish surface coating, the composition of which has not yet been defined.

Finally, atacamite, a basic copper chloride, is present below the brownish-black patina deposits, indicating an electrochemical attack on the alloy in the presence of a chloride ion. This ion accelerates the corrosion and, in certain cases, promotes pitting. Its presence can be attributed either to the airborne chloride deposits (marine particulate, emissions from the combustion of plastics containing chlorine), or to the attack of the surface by chemical compounds containing chlorine.

## Process and Condition of the Gilding

Not all of the tests have been completed for this important and complex monument. Study of the gilding process in particular is still in progress. The first phase of testing involves metallographic analysis of samples taken from the horse and from the mantle of the horseman to obtain information on the thickness of the gold leaf, the stages of application, and the extent of the corrosion process.

Figure 10 shows the metallographic section of one sample: two pieces of gold leaf rest on corrosion products that penetrate to a maximum depth of 0.3 mm; the pieces are completely detached from the metal and separated from each other by the same oxidation products. The thickness of the gold leaf varies from 3 to 9 microns. This measurement is consistent with the values cited by Oddy et al. (1979).

Three other characteristics of the gilding of the monument should be noted: (1) residual gilding is present almost exclusively on the Roman sections and repairs; (2) the surface of the horseman shows minute scoring in definite directions, suggesting that the alloy was textured in this way to anchor the gold leaf more effectively (see the term *concisuris* in Pliny 1961, book XXXIV, chapter 19); and (3) in two areas of the horse's hindquarters, which are covered by the horseman, a series of roughly square gold leaves with sides varying from 5 to 9 cm are visible. A similar square pattern is present on the *Horses of San Marco* (Galliazzo 1981) and on some bronze statues cited by Oddy et al. (1979). In Pliny's treatise two methods of gilding

FIGURE 8. *Damaged gold surface.*

FIGURE 9. *Typical alternation of light and dark areas of surface corrosion.*

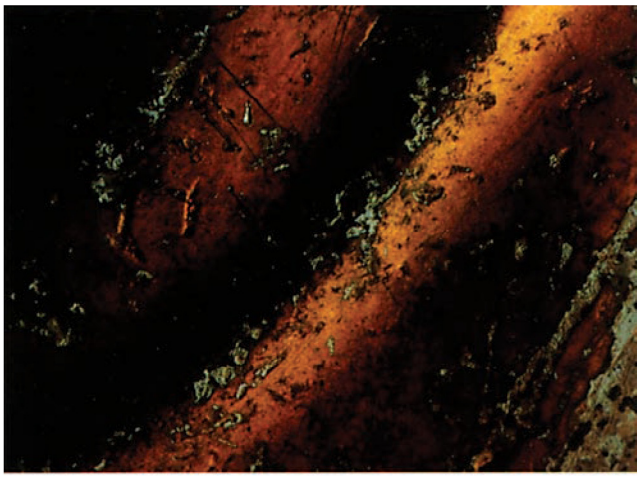

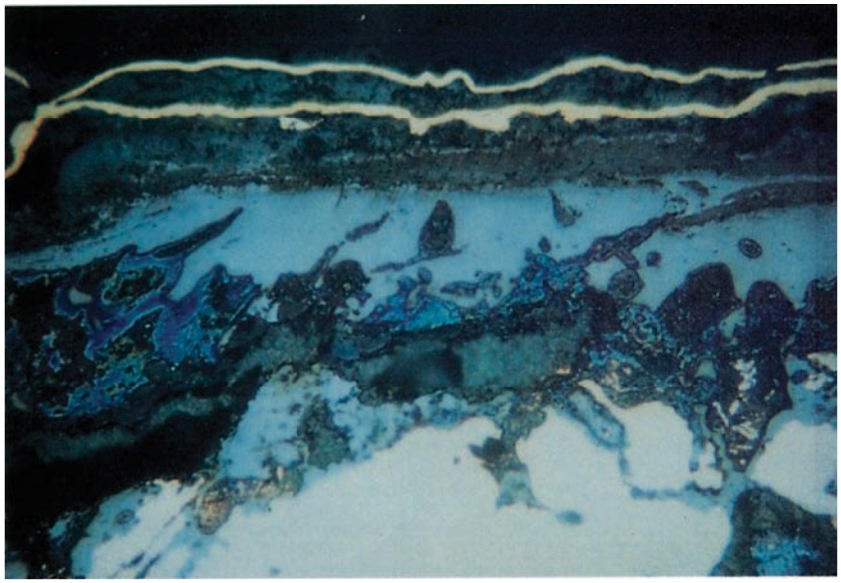

FIGURE 10. *Metallographic section of an alloy specimen from the horse.*

are cited directly (book XXXIII, chapter 20), and a third indirectly (book XXXIV, chapter 19), concerning a bronze statue of Alexander the Great, which the Emperor Nero later had gilded. Basically the methods involve gilding with cold mercury, gilding with proteic glue, and gilding with gold foil or gold leaf (*à l'hache*).

Oddy's hypothesis that fire (mercury) gilding began at the end of the second or beginning of the third century C.E. seems well founded (Oddy 1982). Both Oddy (1982) and Craddock et al. (1987–88) have published lists of bronzes that contain large quantities of tin and lead and were not gilded with mercury. On the other hand, lead bronzes (including the Marcus Aurelius) cannot be gilded with mercury, either by the cold process or the hot process. Therefore, discarding the hypothesis of gilding with proteic adhesive for the Capitoline monument, which was intended to be placed outdoors, only the *à l'hache* technique seems probable. However, the use of this process should be checked against both the analysis of alloy microsamples and the current foundry experiments.

## Observations and Conclusions

During the restoration, several reagents and processes for cleaning the surface were perfected in collaboration with the restorer Paola Fiorentino. The practical experimentation was rather long and laborious, since the objective was essentially to remove the corrosion products on top of the gold without dissolving or detaching those underneath.

ICR and the Selenia Company, working in collaboration, carried out a test of eleven surface coatings for the conservation of bronzes outdoors (Marabelli and Napolitano 1991). At the end of the study, it was possible to establish that the best formula was provided by Incralac or Paraloid B72 as primer and Reswax WH (a mixture of a polyethylene wax and two microcrystalline waxes) as a protective finish.

Despite the studies completed thus far, a product capable of ensuring protection without extensive maintenance for a period of at least twenty to thirty years has not been developed. On the other hand, given the precarious adhesion of the gold,

massive fixative treatments or cyclical surface cleaning are inadvisable for the Marcus Aurelius if it is relocated outdoors. At the present time, therefore, the best and most rational solution for the conservation of the two statues would be a climate-controlled museum environment that provides filtration of the atmospheric pollutants. This does not exclude the future possibility of returning the monument to its original position outdoors, if protection and maintenance operations could be assured with little or no damage to the patina and residual gold.

## References


ACCARDO, G., D. AMODIO, P. CAPPA, A. BENNICI, G. SANTUCCI, AND M. TORRE

1989 Structural analysis of the equestrian monument to Marcus Aurelius in Rome. In *Structural Repair and Maintenance of Historical Buildings,* 581–92. C. A. Brebbia, ed. Southampton, U.K.: Computational Mechanics Institute.

ACCARDO, G., A. BENNICI, M. TORRE, D. AMODIO, P. CAPPA, AND G. SANTUCCI

1989 An experimental study of the strain fields on the statue of Marcus Aurelius. In *Proceedings of the 1989 SEM Spring Conference on Experimental Mechanics*, 534–37. Bethel, Conn.: Society for Experimental Mechanics.

ACCARDO, G., C. CANEVA, AND S. MASSA

1983 Stress monitoring by temperature mapping and acoustic emission analysis: A case study of Marcus Aurelius. *Studies in Conservation* 28:67–74.

ACCARDO, G., F. CAPOGROSSI, G. SANTUCCI, AND M. TORRE

1984 Determinazione del carico. In *Marco Aurelio*: *Mostra di Cantiere*, 60. Rome: Arti Grafiche Pedanesi.

ACCARDO, G., F. DE SANTIS, F. GORI, G. GUATTARI, AND J. M. WEBSTER

1985 The use of speckle interferometry in the study of large works of art. In *Proceedings of the 1st International Conference on Non-destructive Testing in Conservation of Works of Art* 4(1):1–12. Rome: Istituto Centrale per il Restauro (ICR) and Associazione Italiana Prove non Distruttive (AIPnD).

CALEY, E. R.

1970 Chemical composition of Greek and Roman statuary bronzes. In *Art and Technology: A Symposium on Classical Bronzes,* 37–49. Cambridge: MIT Press.

CANELLA, G., M. MARABELLI, A. MARANO, AND M. MICHELI

1985 Esame ultrasonoro della statua equestre del Marco Aurelio. In *Proceedings of the 1st International Conference on Non-destructive Testing in Conservation of Works of Art* 1(8):1–12. Rome: Istituto Centrale per il Restauro (ICR) and Associazione Italiana Prove non Distruttive (AIPnD).

CRADDOCK, P. T., B. PICHLER, AND J. RIEDERER

1987–88 Legierungszusammensetzung in naturwissenschaftliche Untersuchungen an der Bronzestatue Der Jüngling vom Magdalensberg. *Weiner Berichte über Naturwissenschaft in der Kunst* 4(5):262–95.

DE LACHENAL, L.

1989 Il monumento nel Medioevo fino al suo trasferimento in Campidoglio. In *Marco Aurelio: storia di un monumento e del suo restauro*, 129–55. Milan: RAS.

FERRETTI, M., R. CESAREO, M. MARABELLI, AND G. GUIDA

1989 The analysis of bronze alloys from the equestrian statue of Marco Aurelio by means of a thin sample XRF technique. *Nuclear Instruments and Methods in Physics Research* B 36:194–99.

FIORENTINO, P.

1989 La doratura: Note sulle tecniche di esecuzione e osservazioni sulla superficie del monumento. In *Marco Aurelio: Storia di un monumento e del suo restauro*, 263–77. Milan: RAS.

FITTSCHEN, K.

1989 Il ritratto del Marco Aurelio: considerazioni, critiche dopo il restauro. In *Marco Aurelio: Storia di un monumento e del suo restauro*, 75–78. Milan: RAS.

GALLIAZZO, V.

1981 *I cavalli di S. Marco*. Treviso: Canova.

GRAEDEL, T. E.

1987 Copper patinas formed in the atmosphere III. *Corrosion Science* 27(7)[special issue]:741–69.

LECHTMAN, H., AND A. STEINBERG

1970 Bronze joining: A study in ancient technology. In *Art and Technology: A Symposium on Classical Bronzes,* 5–35. Cambridge: MIT Press.

MARABELLI, M.

1979 *Scheda di analisi* 684. Rome: ICR.

1992 The environment and the future of outdoor bronze sculpture: Some criteria of evaluation. In *Proceedings of "Dialogue 89."* Baltimore: National Association of Corrosion Engineers (NACE).

MARABELLI, M., A. MARANO, S. MASSA, AND G. VINCENZI

1988 La condensazione capillare di vapore acqueo in patine di bronzi esposti all'aperto. In *Preprints of the 2d International Conference on Non-destructive testing, Microanalytical Methods and Environment Evaluation for Study and Conservation of Works of Art* 2(25):1–20. Rome: ICR and AIPnD.

MARABELLI, M., AND G. NAPOLITANO

1991 Nuovi sistemi protettivi applicabili su opere o manufatti in bronzo esposti all'aperto. *Materiali e Strutture* 1(2):51–58.

MEDORI, M.

1983 Utilizzazione del piano di impedenza nelle ispezioni Eddy Current. In *Preprints: Conferenza nazionale Prove non Distruttive,* 1–25. Brescia: AIPnD.

MICHELI, M.

1989 Le tecniche di esecuzione e gli interventi di riparazione. In *Marco Aurelio: Storia di un monumento e del suo restauro*, 253–62. Milan: RAS.

ODDY, W. A.

1982 Gold in antiquity: aspects of gilding and of assaying. *The Journal of the Royal Society of Arts* (October):1–14.

ODDY, W. A., L. BORRELLI VLAD, AND N. D. MEEKS

1979 The gilding of bronze statues in the Greek and Roman World. In *The Horses of San Marco, Venice,* 182–87. G. Perocco, ed. Milan and New York: Olivetti.

PICON, M., S. BOUCHER, AND J. CONDAMIN

1966 Recherches techniques sur des bronzes de Gaule Romaine I. *Gallia* XXIV (1):189–215.

PICON, M., J. CONDAMIN, AND S. BOUCHER

1967 Recherches techniques sur des bronzes de Gaule Romaine II. *Gallia* XXV (1):153–68.

1969 Recherches techniques sur des bronzes de Gaule Romaine III. *Gallia* XXVI (2):245–78.

PLINIUS DER ÄLTERE

1985 *Über Kupfer und Kupferlegierungen, herausg: Projektgruppe Plinius 1984.* Essen: Verlag Gluckauf.

PLINY THE ELDER

1961 *Natural History*. Reprint. London: Heinemann.

STEINBERG, A.

1973 Joining methods on large bronze statues: Some experiments in ancient technology. In *Application of Science in Examination of Works of Art: proceedings of the seminar: June 15–19, 1970,* 103–37. Boston: Museum of Fine Arts.

TORELLI, M.

1989 Statua Equestris Inaurata Caesaris: mos e ius nella statua di Marco Aurelio. In *Marco Aurelio: storia di un monumento e del suo restauro,* 83–102. Milan: RAS.

## BIOGRAPHY

Maurizio Marabelli, chemist, is head of the Chemistry Laboratory at the Istituto Centrale del Restauro (ICR) in Rome, where he teaches chemistry at the ICR School of Restoration. He also teaches chemistry of restoration at the Faculty of Conservation of Cultural Property, University of Tuscia, Viterbo. Dr. Marabelli is the author of more than ninety papers in the fields of nondestructive technology, conservation of metals and mural paintings, and air-pollution control.